Advanced Lookup Table for Enhanced Maximum Power Point Tracking Accuracy in Photovoltaic Systems

Flavius Maxim PETCUT

Faculty of Engineering, Aurel Vlaicu University of Arad,
Arad, Romania, (flavius.petcut@uav.ro)

Abstract: Efficient Maximum Power Point Tracking (MPPT) techniques play a vital role in optimizing energy extraction from photovoltaic (PV) systems, primarily due to the high sensitivity of photovoltaic panel (PVP) characteristics to varying environmental parameters, including ambient temperature and solar irradiance. Conventional MPPT methods generally depend on identifying and following reference points, which are extracted from variables closely related to the Maximum Power Point (MPP) on the external current-voltage $I(V)$ characteristics of PVP. In response to the limitations inherent to traditional approaches, this study proposes an advanced lookup table strategy to generate highly accurate reference values explicitly as functions of measured ambient temperature and solar irradiance. Initially, this research employs the two-diodes electrical circuit model to rigorously define the foundational relationships between ambient temperature, irradiance, and photovoltaic panel performance. Subsequently, contemporary advanced extraction methods based on recent academic literature were applied, enabling accurate identification of the MPP coordinates. Creating an effective lookup table requires comprehensive and detailed experimental datasets, which are often insufficient or unevenly distributed in practical scenarios. To address this challenge, the Shepard global interpolation method was integrated into the model development process, effectively mitigating datasets limitations through accurate interpolation of missing data points. This approach significantly elevates the precision and robustness of MPPT models. A comprehensive case study, conducted with real-world experimental datasets, rigorously validated the accuracy and reliability of the proposed interpolation-based lookup table. The results confirm substantial enhancements in MPPT accuracy, facilitating greater energy extraction efficiency and improved overall performance in practical photovoltaic applications.

Keywords: Photovoltaic panel (PVP), Power Point Tracking (MPPT), Lookup table, Shepard global interpolation.

1. INTRODUCTION

Accurate Maximum Power Point Tracking (MPPT) is fundamental to maximizing the efficiency of photovoltaic (PV) energy systems, as it determines the optimal operating condition at which solar panels can deliver their maximum achievable power output. Achieving this optimal point ensures the best possible energy yield from the solar array under prevailing environmental conditions. Conventional MPPT techniques predominantly rely on the extraction of reference points derived from the external current–voltage (I–V) characteristics of photovoltaic panels (PVP), as demonstrated by Saberi et al. (2023), Ananda-Rao Able et al. (2020), and Able et al. (1954). While these classical methods, including Perturb and Observe (P&O) and Incremental Conductance (IncCond), are widely implemented due to their simplicity and relatively low computational demands, they are often hindered by inherent performance limitations. In particular, their accuracy is compromised by a limited capacity to adapt in real time to variations in environmental parameters such as ambient temperature, fluctuating solar irradiance, and complex partial shading conditions Zaghba et al. (2024). Additional approaches, such as mobile PV panel tracking systems Lourido et al. (2024), have been explored to increase sun exposure but do not fully resolve MPPT under non-uniform conditions.

To overcome these challenges, modern research has increasingly shifted towards intelligent MPPT techniques based on soft computing and metaheuristic optimization algorithms. Notable among these are Particle Swarm Optimization (PSO), Genetic Algorithms (GA), Artificial Neural Networks (ANN), Fuzzy Logic Controllers (FLC), and the Firefly Algorithm (FA). PSO and GA emulate natural swarm and evolutionary behaviors, respectively, to locate the global maximum power point more efficiently under complex irradiance patterns. ANN-based approaches use trained models to predict the MPP based on environmental input parameters, while FLC employs linguistic rules to handle system uncertainties and non-linearity without requiring an accurate mathematical model. The Firefly Algorithm, inspired by the bioluminescent communication of fireflies, has recently demonstrated promising results in global optimization tasks, including tracking the global MPP in multi-peak I–V curves generated under partial shading.

Building on this trend, the present study proposes an advanced MPPT strategy that integrates novel lookup table methodologies enhanced by intelligent control logic Ichim-Burlacu et al. (2024), Dragomir et al. (2013), Korodi et al. (201). These models utilize extensive datasets collected across a broad range of operating conditions and are combined with adaptive algorithms capable of learning and adjusting in real time. The objective is to improve MPPT performance by increasing precision, responsiveness, and adaptability, particularly under fast-changing or highly variable conditions. This approach not only aims to optimize energy output but also enhances overall system reliability, operational stability, and resilience to environmental disturbances Ulaganathan et al. (2023), Dragomir et al. (2010a). As such, it represents a significant advancement over traditional methods, aligning with current trends in smart PV system design.

2. MODEL USED TO EMULATE THE PHOTOVOLTAIC PANEL

2.1 Equivalent two-diodes circuit diagram

On the paper, to emulate the photovoltaic panel on use the extended two-diodes model, presented on Fig. 1. This study addresses these limitations by proposing advanced lookup table strategies designed to improve MPPT accuracy. The proposed method for determining the MPP of the external $I(V)$ characteristic of a photovoltaic panel was presented in Dragomir et al. (2013), Korodi et al. (2011), Dragomir et al. (2010a), Petcut et al. (2010).

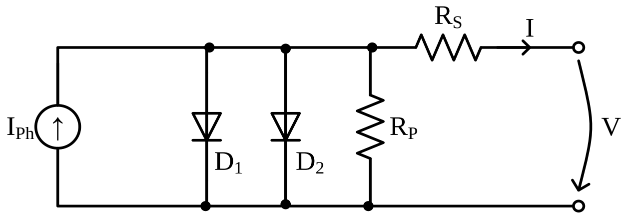

Figure 1. Equivalent two-diodes circuit diagram of a PVP.

2.2 Mathematical equivalent two-diodes circuit diagram

The method used in this research is based on the assumption that the solar panel has the equivalent of the two-diodes electrical circuit model from Fig. 1, respectively an external characteristic $I(V)$ with the mathematical model.

$$I = I_{ph} - I_{01}\left(e^{\frac{V+I\cdot R_S}{V_{T1}}} - 1\right) - I_{02}\left(e^{\frac{V+I\cdot R_S}{V_{T2}}} - 1\right) - $$

$$- \frac{V + I \cdot R_S}{R_P}, \text{for } \theta = constant, G = constant. \quad (1)$$

Using genetic algorithms (GA), advanced extraction techniques, we can calculate all the 7 parameters of the model - Light-generated current I_{Ph}, Reverse bias saturation currents I_{01}, I_{02}, Series resistance R_S, Parallel resistance R_P, Voltages associated to temperature influence V_{T1} and V_{T2}- from experimental characteristics $I(V)$ Dragomir et al. (2010a), Petcut et al. (2010).

The efficiency of PV energy systems critically depends on accurately tracking the MPP, which represents the optimal work for solar panel to deliver their maximum achievable power output. Traditional MPPT methodologies primarily rely on extracting reference points of the external $I(V)$ characteristics of PVP Ahmed er al. (2020). These conventional methods frequently exhibit performance limitations, particularly inaccuracies arising from their restricted responsiveness to real-time variations in environmental parameters such as ambient temperature fluctuations, dynamic solar irradiance levels, and partial shading scenarios. Such environmental conditions significantly influence the PVP electrical characteristics, thereby impacting overall energy conversion efficiency.

The MPPT type systems are designated to obtain the maximum power from the PVP by ensuring that they consistently operate at their MPP of the PV systems (Fig. 2).

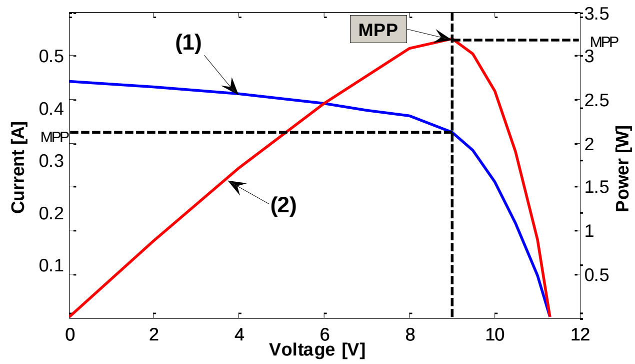

Figure 2. PVP characteristic $I(V)$ - (1),
PVP characteristic $P(V)$ - (2).

In this paper, to generate the reference values for MPPT type systems, lookup table are applied. Depending on the parameters θ and G, considered as input values, the lookup table provides the values of the MPP of the power P_M. Corresponding to the value of the MPP we have corresponding current: I_M and the corresponding voltage value of the MPP – V_M. Using transcendent equation (1), we can obtain the MPP, from the relation (2).

$$P_M = I_M \cdot V_M \quad (2)$$

The use of the models (1) and the method from Dragomir et al. (2010a) for extracting the MPP do not constrain the application of the lookup table. For example, the lookup table can also be generated based on quasi-empirical models Dragomir et al. (2013). A concise overview of the lookup table's background is provided in Kchaou et al. (2017), Yue et al. (2023), and Yue et al. (2021).

To generate the above-mentioned lookup table, it is essential to have a set of experimentally determined external characteristics $I(V)$. Extensive research on photovoltaic systems and numerous manufacturers in the market have significantly increased the availability of relevant data. In the current work, a PV system comprising a solar panel has been employed to update and validate the models, aligning with contemporary technologies and data availability. Additionally, the global interpolation procedure described in Dragomir et al. (2013) was adopted for designing reference interpolation point of controllers.

The idea to use lookup tables for Maximum Power Point Tracking (MPPT) in photovoltaic (PV) systems has been explored in various studies, including those by Petcut et al. (2010) and Yue et al. (2021).

In Petcut et al. (2010) was studied the lookup table for MPPT was initially discussed in the context of the external characteristics of the PV system rather than directly targeting the MPP. This approach involves using predefined data to estimate the optimal operating points based on external conditions such as irradiance and temperature.

Further details on the use of lookup tables for MPPT are provided by Yue et al. (2021), emphasizing the integration of lookup tables with other MPPT methods to enhance performance. For instance, combining lookup tables with the P&O method allows for quick approximation of the MPP, followed by fine-tuning using P&O.

In section II of the paper, the method used to determine the coordinates for MPP is summarized based on Dragomir et al. (2010a). In Section III are presented the proposed look up models. In this section it is, also, indicated how the lookup table can be integrated into a MPPT structure. Finally, the last section discusses the main conclusions of the paper.

3. DETERMINATION OF MPP COORDINATES

Considering known the external characteristic (1) of the solar panel, the MPP coordinates, V_M, I_M, may be obtained by solving the system:

$$F_1(V_M, I_M) = 0, \quad F_2(V_M, I_M) = 0 \tag{3}$$

where:

$$F_1(V,I) = V - I_{Ph}\cdot R_P + I_{01}\cdot R_P\cdot\left(e^{\frac{V+I\cdot R_S}{V_{T1}}} - 1\right) + I_{02}\cdot R_P \cdot\left(e^{\frac{V+I\cdot R_S}{V_{T2}}} - 1\right) + (R_S + R_P)\cdot I$$

$$F_2(V,I) = 1 + R_S\cdot\left(\frac{I_{01}}{V_{T1}^2}\cdot(V_{T1} + I\cdot R_S - V)\cdot e^{\frac{V+I\cdot R_S}{V_{T1}}} + \quad + \frac{I_{02}}{V_{T1}^2}\cdot(V_{T2} + I\cdot R_S - V)\cdot e^{\frac{V+I\cdot R_S}{V_{T2}}} + \frac{1}{R_P}\right)$$

Both equations (3) are classified as Lambert-type equations, a category of transcendental equations characterized by the presence of variables both in the base and in the exponent, often in the form $x = ae^{bx}$. Such equations frequently arise in the analytical modelling of PV cells, particularly when describing the C–V relationship of single or multi-diode models. In the context of PV systems, solving these equations explicitly is notably challenging due to their nonlinearity and the presence of exponential terms tied to both voltage and current.

Given the mathematical complexity and computational burden associated with solving Lambert-type equations directly, an alternative approach was adopted. Rather than attempting to analytically or numerically solve system (3) in its original form, Dragomir et al. (2010a) proposed the use of an associated dynamical system, denoted as system (4). This reformulation describes the PV system using a second-order dynamic model, where the state variables are the voltage V and the current I. By recasting the static nonlinear algebraic system into a time-dependent differential system, the problem becomes more tractable for simulation-based methods, such as those implemented in Simulink. This approach facilitates the determination of the system's steady-state behavior through time-domain analysis, effectively bypassing the need to directly resolve the Lambert expressions while still capturing the essential dynamics and equilibrium points of the original system.

$$\frac{dV}{dt} = -k_1\cdot F_1(V,I), \quad \frac{dI}{dt} = -k_2\cdot F_2(V,I) \tag{4}$$

Here, k_1 and k_2, are two parameters used to control the speed integration and F_1 and F_2. This auxiliary's functions are used to determine the coordinates of the MPP.

It was demonstrated that within the domain of interest, $[0, V_0]$ x $[0, I_{SC}]$ (V_0- open circuit voltage, I_{SC} - short circuit current), the system exhibits asymptotic stability at its equilibrium point. At this point, system (4) simplifies to the form of equation (3), yielding the values V_M and I_M associated with the MPP operating condition. In order to solve the dynamical system (4) was used the Simulink model from Fig. 3 Dragomir et al. (2010b). The results obtained for an external characteristic as in Fig. 2 were illustrated the variation of the current in Fig. 4 and the variation of the voltage in Fig.5, with the model parameters from (5):

$$I_{01} = 138.844\cdot 10^{-12}\,A, I_{02} = 25.921\cdot 10^{-9}\,A,$$
$$I_{ph} = 0.458832\,A,$$
$$R_S = 2.5893\,\Omega, R_P = 131.922\,\Omega,$$
$$V_{T1} = 0.520635\,V, V_{T2} = 0.972031\,V. \tag{5}$$

The plotted results are associated to the initial state $V(0) = 4\,V, I(0) = 0.4\,V$ Dragomir et al. (2010b).

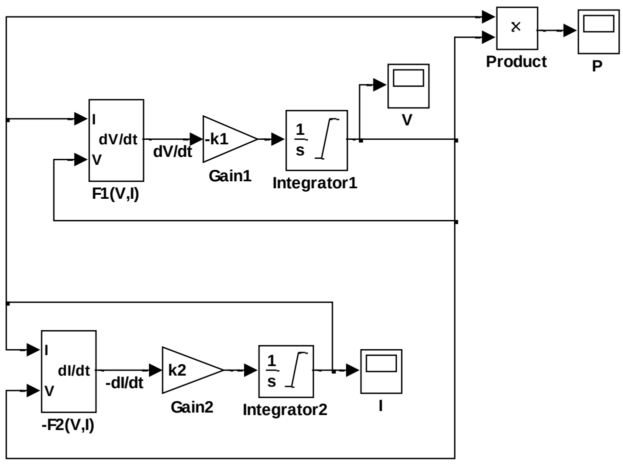

Figure 3. The method used to determine the steady-state regime of system, with Simulink model (4).

The diagram from Fig. 3 shows two subsystems corresponding to the differential equations that govern the voltage and current evolution over time. The simulation helps in understanding how the PV system reaches steady-state for a given set of initial conditions and parameters.

The obtained current are presented in Fig. 4 and the obtained voltage are presented in Fig.6. As we can see on the, the stabilisation time is 2 second, thet is lass thet the variation of the G or θ.

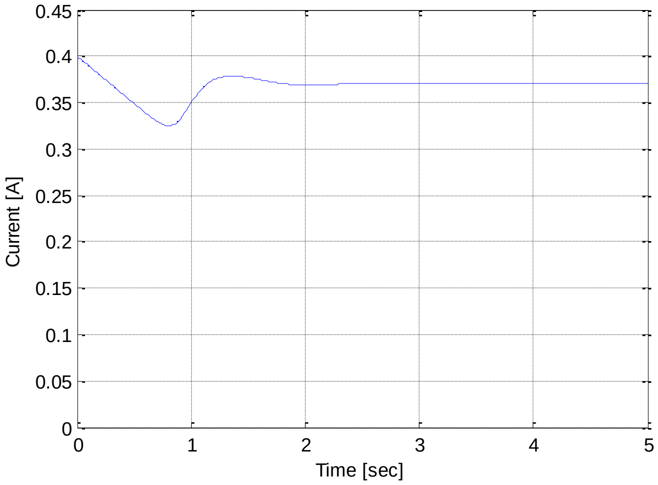

Figure 4. $I(t)$ variation of the current for $V(0) = 4\ V$ and $I(0) = 0.4\ A$ leads to $I_M = 0.373\ A$.

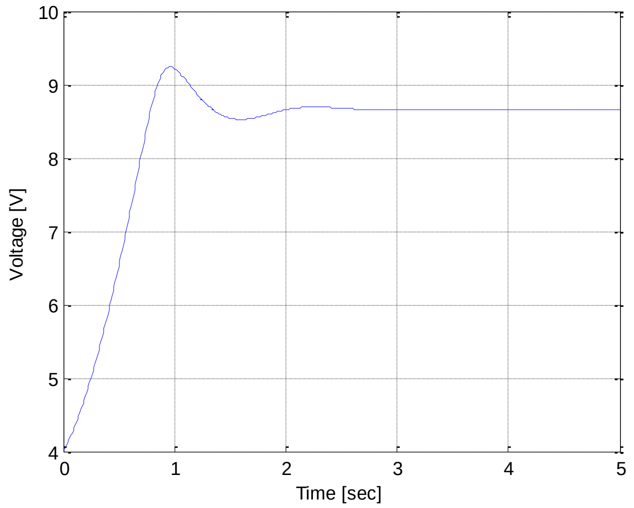

Figure 5. $V(t)$ the variation of the voltage for $V(0) = 4\ V$ and $I(0) = 0.4\ A$ leads to $I_M = 0.373\ A$.

4. THE DESIGN AND USE OF LOOKUP TABLE

To use MPPT strategies, is require the knowledge the values of I_M and/or V_M, to use these as references values Korodi et al. (2011), Dragomir et al. (2010a). When we have the variation of the parameters θ and G of the characteristic (1), as well as the values of the parameters I_M, V_M and P_M, change in the current operation regimes. By using two-dimensional lookup table provided by relation (6):

$$I_M = f_1(\theta, G), V_M = f_2(\theta, G), P_M = f_3(\theta, G) \qquad (6)$$

the obtaining of I_M, V_M and P_M as functions of θ and G can be simplified. In (5), f_1, f_2 and f_3 are interpolation functions. Identifying this function requires knowledge of various external characteristics $I(V)$ of the solar panel, experimentally determined for different values of the parameters θ and G. As mentioned in the introduction, the literature on this topic is limited. In this context, for the case study presented below, the characteristics from Kchaou et al. (2017) were used in Fig. 6 and Fig. 7.

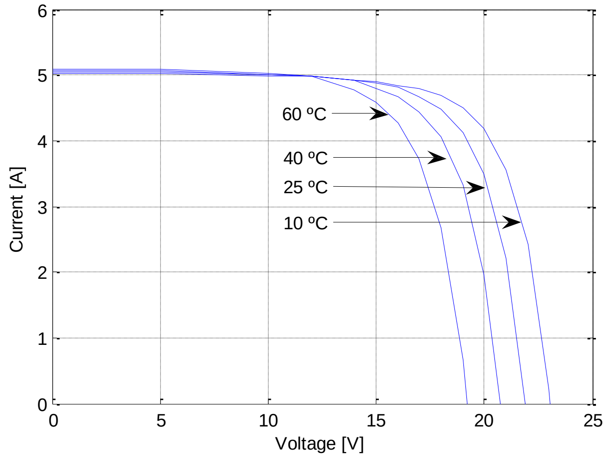

Figure 6. $I(V)$ characteristics displayed for different temperature levels.

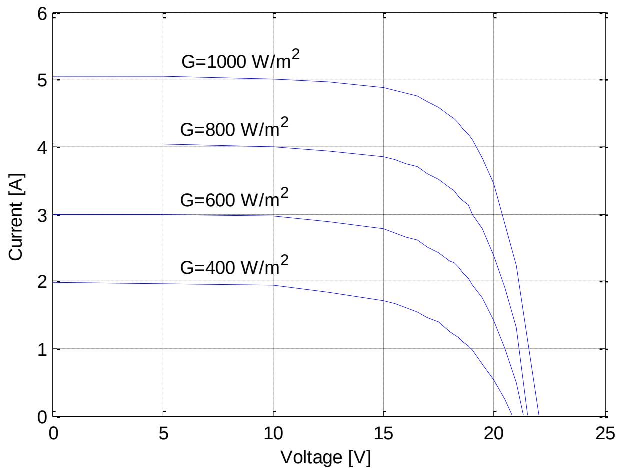

Figure 7. $I(V)$ characteristics displayed for different irradiance levels.

Several steps are required to obtain the models (5):

Step I: Using the GA-based method described in Petcut et al. (2010) we identified the 7 parameters of the model (1) for each of these characteristics.

Step II: For each model obtained in Step I, we calculated the MPP coordinates using the method from Dragomir et al. (2010a) and the Simulink diagram presented on Fig. 3. The results are presented in Table 1 Dragomir et al. (2010b). After comparing the values from the results with those that we extracted directly from the characteristics in Petcut et al. (2010), we confirm the accuracy of both model (1) with GA-determined parameters and the MPP determination method.

For beginning, the corresponding Cartesian grids for each of the three interpolation models are extracted from Table 1.

Step III: Starting from Table 1 the interpolative models (5) are generated.

Since each grid contains only seven support points of the type $I_M(\theta, G)$, $V_M(\theta, G)$ and $P_M(\theta, G)$ they are incomplete. The next-$I_M(\theta, G)$, $V_M(\theta, G)$ and $P_M(\theta, G)$ they are incomplete.

Table 1 Initial grid of I_M and V_M

θ[C] / G[Wm^{-2}]	10		25		40		60	
	I_M	V_M	I_M	V_M	I_M	V_M	I_M	V_M
400			1.58	16.2				
600			2.52	17.5				
800			3.46	18.2				
1000	4.34	19.7	4.31	18.8	4.26	17.8	4.20	16.4

The next step involves completing the Cartesian grids using an interpolation method, in our study we used the Shepard interpolation.

We selected this method, as discussed in Yue et al. (2021), due to its excellent properties, such as smoothness and global interpolation, as well as the favorable results it has yielded in designing Reference Interpolation Point - RIP controllers.

Shepard interpolation provides the support values of V_M, I_M or P_M in this case for an incomplete support point (current point) within the Cartesian grid. The support value at a given point with coordinates (θ, G), is determined based on its position relative to all completed points in the grid. Let n_s represent the number of these completed points (i.e., the number of external experimental characteristics used to generate the lookup table). The Shepard interpolation formula is given by (7):

$$c = \frac{\left(\sum_{i=1}^{n_s} w_i \cdot c_i\right)}{\left(\sum_{i=1}^{n_s} w_i\right)},$$

$$w_i = \left[\sqrt{(\theta - \theta_i)^2 + (G - G_i)^2}\right]^{-\mu} \quad (7)$$

where: $c = I_M, V_M$ or P_M represents the support value of the current point,c_i represents the support value of a complete support point with the coordinates (θ_i, G_i), and w_i represents the weight associated to coordinates pairs $\{(\theta, G), (\theta_i, G_i)\}$. The weight w_i is inversely proportional with the exponential μ of the distance between the support places $(\theta, G)$and (θ_i, G_i). In our case, we used $\mu = 1.5$.

Given that a grid with only 16 support points is relatively sparse, we further extended each grid using the Shepard interpolation method. As a result, the Cartesian grids presented in Table 2 were obtained Dragomir et al. (2010b).

Table 2 Extended Cartesian grid of I_M and V_M

θ[C] / G[Wm^{-2}]	10		20		25		30	
	I_M	V_M	I_M	V_M	I_M	V_M	I_M	V_M
400	1.66	16.3	1.59	16.2	1.58	16.2	1.60	16.2
600	2.57	17.5	2.53	17.5	2.52	17.5	2.53	17.5
800	3.49	18.2	3.46	18.2	3.46	18.2	3.47	18.2
1000	4.34	19.7	4.29	18.9	4.31	18.8	4.29	18.6

θ[C] / G[Wm^{-2}]	40		50		60	
	I_M	V_M	I_M	V_M	I_M	V_M
400	1.66	16.3	1.75	16.3	1.84	16.4
600	2.57	17.5	2.63	17.5	2.68	17.5
800	3.49	18.2	3.52	18.1	3.55	18.1
1000	4.26	17.8	4.24	17.4	4.20	16.4

Step IV: The extended grids generated in the previous step can be implemented as a lookup table using different interpolation methods. For current Fig. 8 and for volage Fig. 9 illustrates the results obtained through the Lookup Table block in the Simulink platform. Notably, the surfaces $I_M(\theta, G)$ and $P_M(\theta, G)$demonstrate a significant level degree of flatness.

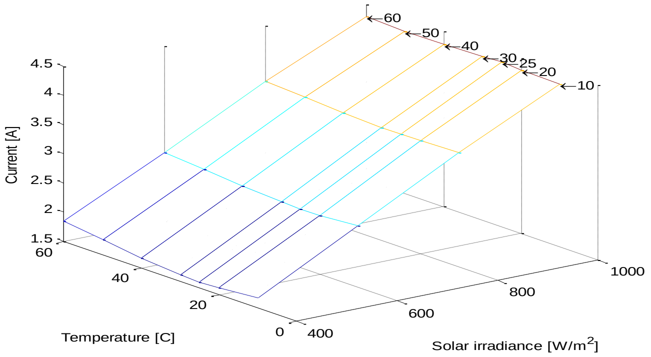

Figure 8. $I_M = f_1(\theta, G)$ models obtained with Simulink Lookup table.

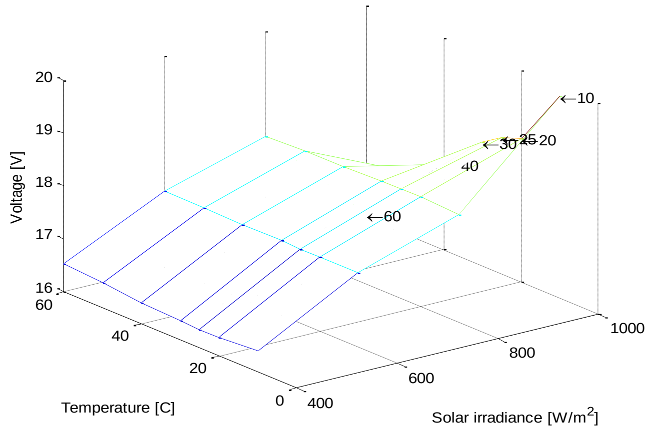

Figure 9. $V_M = f_2(\theta, G)$ models obtained with Simulink Lookup table.

The principle of use of the lookup table in a MPPT logical structure of photovoltaic panel emulator is presented in Fig. 10.

The interpolative blocks $f_1(\theta, G)$ and $f_2(\theta, G)$ are design particularly for each application and provide, based on the values of θ and G, the reference values of I_M and/or V_M to the controller that drives the DC/DC converter. $S - \theta$ and $S - G$ are the temperature and solar radiation sensors.

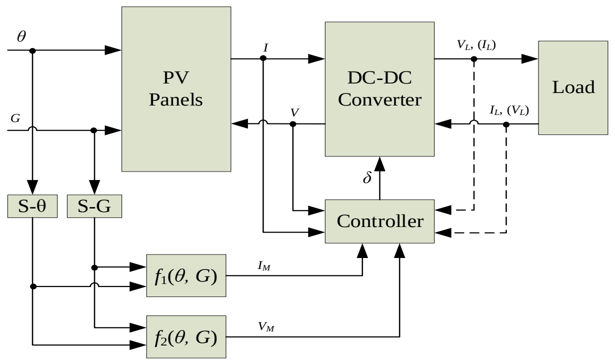

Figure 10. Logical structure of photovoltaic panel emulator.

The figure illustrates a boost-type DC-DC converter connected to a photovoltaic (PV) module with an unspecified load, forming a simplified representation of a typical PV power conditioning system. Because the subject of this paper is not detailing with MPPT strategies, the interested readers can use for this purpose the papers Saberi et al. (2023) and Petcut et al. (2010). While this work does not implement an optimization routine, it acknowledges the importance of real-time power extraction methods in enhancing PV system efficiency. For future developments aimed at improving energy yield, particularly in systems with dynamic environmental exposure, mobile solar panel configurations as discussed in Ulaganathan et al. (2023) may present a promising direction for further investigation.

5. EXPERIMENTAL BOARD TO EMULATE A PHOTOVOLTAIC PANEL

The experimental setup used for the validation is illustrated in Fig. 10 have conceptual physical realization presented in Fig. 11.

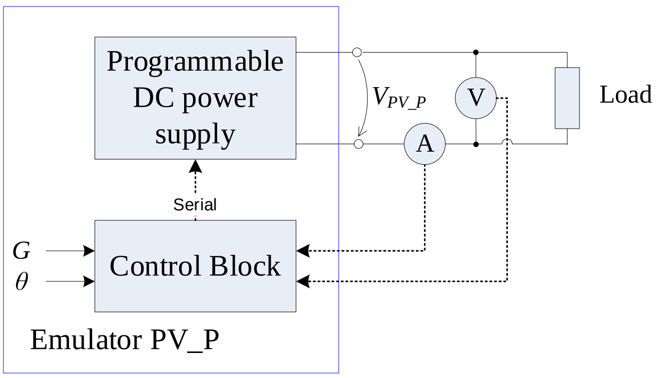

Figure 11. Conceptual physical realization of logical structure of photovoltaic panel emulator.

The fisical realisation of the emulation are prezented in Fig. 12 and was done using an Power Supplay Extech 32280 [Extech 32280] programmable voltage source controlled by a dSPACE DS1103 [DS1103] board. The block diagram is shown in Fig. 12. The PC is required to upload the code to the dSPACE board and to monitor the process.

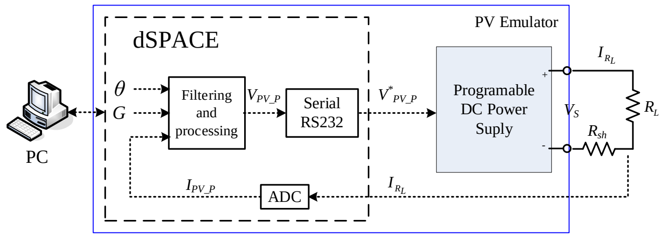

Figure 12. Conceptual physical realization of logical structure of photovoltaic panel emulator with dSpace implementation.

The Simulink physical realization of logical structure of photovoltaic panel emulator using Matlab-Simulink are presented on Fig. 13 and was made using a dSPACE board.

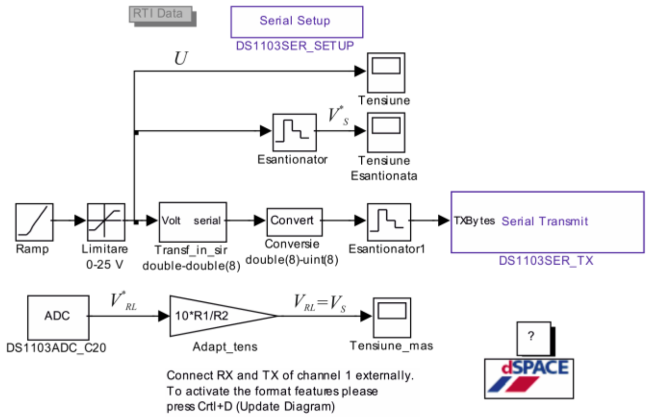

Figure 13. Physical realization of logical structure of photovoltaic panel emulator using Matlab-Simulink.

The result for temperature 25˚C and Sun radiation variations are presented in Fig. 14 and Fig. 15

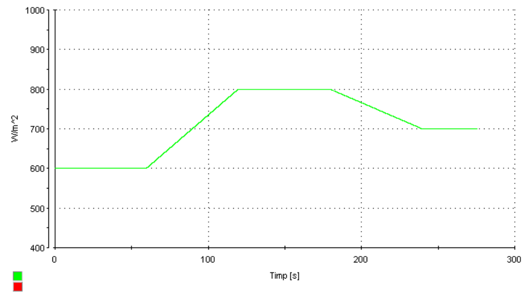

Figure 14 Emulator at Sun radiation variation from 600 W/m2, to 800 W/m2 and return at 700 W/m2.

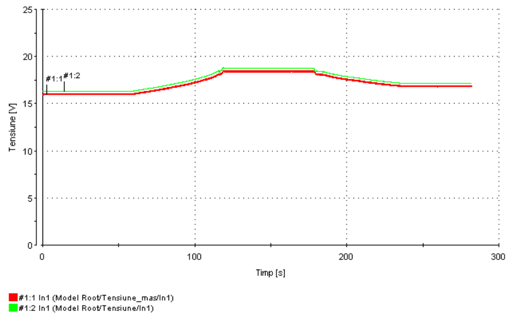

Figure 14 Physical response of the Emulator at Sun radiation variation from 600 W/m2, to 800 W/m2 and return at 700 W/m2.

The system is designed to replicate realistic operating conditions and evaluate the effectiveness of the proposed advanced lookup table in enhancing MPPT accuracy. The setup includes a PV module exposed to controlled environmental parameters, specifically solar irradiance G and the temperature of the photovoltaic panel θ, which are used as key input variables for the MPPT algorithm. These parameters influence the electrical characteristics of the PVP and are crucial in determining the actual operating point at any given moment.

The DC-DC conversion group, integrated within the experimental platform, plays a critical role in adapting the energy harvested from the PVP to match the requirements of the electrical load. This conversion stage ensures that the load L receives a voltage V_L and current $I_L$corresponding to the optimal operating point, which is continuously updated based on the prevailing environmental conditions. Fig. 8 and Fig. 9 offers an additional view of the experimental board, highlighting its modular structure and the integration of measurement, control, and conversion components.

With the assistance of a real-time controller and the proposed advanced lookup table, the system dynamically identifies the Maximum Power Point (MPP), yielding the corresponding optimal current I_M and voltage V_M. This capability ensures that energy extraction from the PV panel is consistently maximized, even under rapidly changing irradiance and temperature conditions.

As a direction for future development, the proposed lookup table methodology can be extended and adapted to mobile PV systems, such as solar-powered vehicles or portable off-grid units. Inspired by the approach of Ulaganathan et al. (2024), this would involve integrating orientation and motion parameters into the lookup table logic, allowing for even more precise MPPT performance in dynamic environments.

6. CONCLUSIONS

This study introduces the development and validation of advanced lookup table designed to accurately determine the maximum power point (MPP) coordinates in photovoltaic (PV) panels, resulting in a notable enhancement in maximum power point tracking (MPPT) performance. These models outperform traditional MPPT techniques primarily due to their dynamic adaptability to variations in ambient temperature and solar irradiance.

A key contribution was defining precise relationships between environmental conditions: ambient temperature and solar irradiance, and PV panel electrical performance, using an advanced two-diodes electrical circuit model. This robust theoretical foundation greatly improved accuracy in predicting PV panel behavior, enabling more efficient energy extraction.

Implementing accurate lookup table requires extensive, detailed experimental datasets, which are often difficult to comprehensively collect. This research addressed data scarcity by employing the Shepard global interpolation method to interpolate missing data points effectively. This innovation significantly increased the models' robustness and practical applicability across varied conditions.

Experimental validations using real-world datasets confirmed the effectiveness and accuracy of the interpolation-based models, demonstrating considerable improvements in MPPT accuracy and controller responsiveness under rapidly changing conditions. Compared to conventional approaches, these lookup table consistently delivered superior performance through precise, real-time reference values directly linked to ambient conditions.

The adoption of these advanced lookup table provides significant practical benefits, including enhanced energy extraction efficiency, improved system reliability, and increased overall performance. Their adaptability ensures operation close to the true MPP, notably increasing power output and efficiency. Their robustness under variable and partially shaded environments makes them particularly valuable for complex real-world applications.

Integrating advanced lookup table with Shepard global interpolation within MPPT strategies marks a substantial advancement in PV technology. Future research could explore further improvements, potentially integrating artificial intelligence techniques to elevate photovoltaic energy conversion efficiency.

One limitation of this study is the reliance on relatively small datasets, which may affect the reliability, accuracy, and generalizability of the results. A small dataset can constrain the ability to capture complex and non-linear relationships, introduce biases, and reduce the robustness of the proposed approach. The use of small datasets also increases the risk of overfitting, where the model performs well on the given dataset but struggles with new, unseen data.

As future work, larger and more diverse datasets can be incorporated to enhance the model's performance and ensure broader applicability. Expanding the dataset could involve collecting data from different conditions, environments, or sources to improve variability and representation. The exploration of advanced data augmentation techniques and the generation of synthetic data offer additional means to overcome the limitations posed by constrained datasets. These measures would contribute to a more rigorous and reliable assessment, thereby enhancing the practical utility of the proposed approach.

REFERENCES

Ahmed, M., Abdelrahem, M., Kennel, R., and M. Hackl, C, (2020). "A Robust Maximum Power Point Tracking Based Model Predictive Control and Extended Kalman Filter for PV Systems", International Symposium on Power Electronics, Electrical Drives, Automation and Motion (SPEEDAM), Sorrento, Italy, pp. 514-519.

Ananda-Rao, K., Matar, Y., Baharudin, N.H., Ismail, M.A., and Abdullah, A.M. (2020). Design of MPPT charge controller using zeta converter for battery integrated with solar Photovoltaic (PV) system, Journal of Physics: Conference Series, pp. 1-8.

Dragomir, T.L., Petcut, F.M., and Dragomir, L.E. (2010a). Maximum Power Point Determination for a Photovoltaic Panel using a Simulink Model, 4th International

Workshop on Soft Computing Applications, 15-17 July, Arad, Romania, pp. 221-224.

Dragomir, T.L and Petcut, F.M (2010b). Look Up Models for Maximum Power Point of photovoltaic panels, The V-th International Conference of ASTR, AGIR, Craiova, Romania, pp. 289-296.

Dragomir, T.L., Petcuţ, FM., and Korodi, A. (2013). Reference Value Generator of Maximum Power Point Coordinates of the Photovoltaic Panel External Characteristic, New Concepts and Applications in Soft Computing. Studies in Computational Intelligence, vol 417. Springer, Berlin, Heidelberg.

DS1103 Used Data acqisition board https://ee.bradley.edu/projects/proj2009/dscntrl/Tutorial.pdf

Extech 32280 Serial programable power supply : https://assets.testequity.com/te1/Documents/pdf/extech/manuals/382280_UM.pdf

Ichim-Burlacu, C., Rat, C. L., and Panoiu, M. (2024). A Look at Lookup Tables as PV MPPT Methods, In 6th Global Power, Energy and Communication Conference, No. 6, (GPECOM), Budapest, Hungary, pp. 51-56.

Korodi, A., Petcut F. M., and Dragomir T. L. (2011) "Interpolative based implementation of a photovoltaic panel," 19th Mediterranean Conference on Control & Automation (MED), Corfu, Greece, pp. 345-350.

Kchaou, A., Naamane, A., Koubaa, Y., and Sirdi, N.K.M' (2017), Review of Different MPPT techniques for a Photovoltaic Generation System, Journal of Automation & Systems Engineering, pp. 195-207.

Lourido,W.N., (2024). Acosta, L.A.C., and Pérez, W.S.A., Design and Implementation of a Prototype Sunflower-Type Photovoltaic System, Journal of Control Engineering and Applied Informatics, Vol. 26, No. 1, pp. 93-103.

Petcut, F.M. and Dragomir, T.L. (2010), Solar Cell Parameter Identification Using Genetic Algorithms, Journal of Control Engineering and Applied Informatics, vol. 12, No.1, pp. 30-37.

Saberi, A., Niroomand, M., and Dehkordi, B.M. (2023). An Improved P&O Based MPPT for PV Systems with Reduced Steady-State Oscillation, International Journal of Energy Research, pp 1-15.

Salman, S., Xin, A.I., and Zhouyang, W.U. (2018). Design of a P-&-O algorithm based MPPT, Protection and Control of Modern Power Systems charge controller for a stand-alone 200W PV system.

Ulaganathan, M., Devaraj, D., and Muniraj, R. (2023). Development of Stand-Alone Photovoltaic System Test-Bed using Neural Network based Solar PV Array Emulator, Journal of Control Engineering and Applied Informatics, Vol.25, No. 3, pp. 55-64.

Yue, X., Geng, D., Chen, Q., Zheng, Y., Gao, G., and Xu, L. (2021). 2-D Lookup Table Based MPPT: Another Choice of Improving the Generating Capacity of a Wave Power System, Renewable Energy, Vol. 179, pp. 625–640.

Yue, X., Meng F., Tong, Z., Chen Q, and Geng, D, Liu J. (2023). Implementation Process Simulation and Performance Analysis for the Multi-Timescale Lookup-Table-Based Maximum Power Point Tracking under Variable Irregular Waves. Energies; 16(22):7501.

Zaghba, L., Khennane Benbitour, M., Fezzani, A., and Borni, A. (2024). Simulation and experimental study of grid-connected photovoltaic power plants in a hot desert climate with fixed and dual-axis tracking. Smart Science, 12(3), pp 407–422.

Appendix A.

Symbol	Representation
$F_1(V,I)$	Auxiliary's functions are used to determine the coordinates of the MPP
$F_2(V,I)$	Auxiliary's functions are used to determine the coordinates of the MPP.
G	Sun radiation
GA	Genetic Algorithm
I	Current
$I(V)$	External current-voltage characteristic
$I(0)$	Current associated to the initial state
I_{01}	Reverse bias saturation currents diode 1
I_{02}	Reverse bias saturation currents diode 2
I_M	Corresponding current value of the MPP
$I_M(\theta,G)$	Support points use to obtain the value of the current MPP
I_{Ph}	Light-generated current
I_{SC}	Short circuit corresponding current
MPP	Maximum Power Point
$MPPT$	Maximum Power Point Trekker
$P\&O$	Perturb and Observe
P_M	The power values of the MPP
$P_M(\theta,G)$	Support points use to obtain the value of the power MPP
PV	Photovoltaic
PVP	Photovoltaic panel
RIP	Reference Interpolation Point
R_P	Parallel resistance
R_S	Series resistance
$S-\mathrm{G}$	Solar radiation sensors.
$S-\theta$	Temperature of the component
V	Voltage
$V(0)$	Voltage associated to the initial state
V_M	Corresponding current value of the MPP
$V_M(\theta,G)$	Support points use to obtain the voltage MPP
V_O	Open circuit voltage
V_{SC}	Short circuit corresponding voltage
V_{T1}	Voltages associated to temperature influence
V_{T2}	Voltages associated to temperature influence
θ	Temperature of solar panel